J|A|C|S
ARTICLES
Published on Web 12/21/2004

Off-Resonance $R_{1\rho}$ NMR Studies of Exchange Dynamics in Proteins with Low Spin-Lock Fields: An Application to a Fyn SH3 Domain

Dmitry M. Korzhnev,[†] Vladislav Yu. Orekhov,[‡] and Lewis E. Kay*,[†]

Contribution from the Protein Engineering Network Centers of Excellence and Departments of Medical Genetics, Biochemistry, and Chemistry, The University of Toronto, Toronto, Ontario, Canada M5S 1A8, and Swedish NMR Center at Göteborg University, Box 465, 405 30 Göteborg, Sweden

Received September 2, 2004; E-mail: kay@pound.med.utoronto.ca

Abstract: An ^{15}N NMR $R_{1\rho}$ relaxation experiment is presented for the measurement of millisecond time scale exchange processes in proteins. On- and off-resonance $R_{1\rho}$ relaxation profiles are recorded one residue at a time using a series of one-dimensional experiments in concert with selective Hartmann−Hahn polarization transfers. The experiment can be performed using low spin-lock field strengths (values as low as 25 Hz have been tested), with excellent alignment of magnetization along the effective field achieved. Additionally, suppression of the effects of cross-correlated relaxation between dipolar and chemical shift anisotropy interactions and ^{1}H−^{15}N scalar coupled evolution is straightforward to implement, independent of the strength of the ^{15}N spin-locking field. The methodology is applied to study the folding of a G48M mutant of the Fyn SH3 domain that has been characterized previously by CPMG dispersion experiments. It is demonstrated through experiment that off-resonance $R_{1\rho}$ data measured at a single magnetic field and one or more spin-lock field strengths, with amplitudes on the order of the rate of exchange, allow a complete characterization of a two-site exchange process. This is possible even in the case of slow exchange on the NMR time scale, where complementary approaches involving CPMG-based experiments fail. Advantages of this methodology in relation to other approaches are described.

Introduction

Protein function often depends on conformational rearrangements occurring on a micro- to millisecond time scale,[1,2] and nuclear magnetic resonance (NMR) spectroscopy is a sensitive tool for the detection and analysis of such processes.[3] In practice, NMR methods for measurement of such dynamics are based on the quantification of line broadening that results from exchange, and two classes of relaxation dispersion experiments have emerged. The first set of experiments involve measurement of the apparent transverse relaxation rate, $R_{2,\mathrm{eff}}$, as a function of the delay between refocusing pulses in Carr−Purcell−Meibum−Gill (CPMG)-type sequences.[4,5] The second class of experiment measures the rotating-frame relaxation rate, $R_{1\rho}$, as a function of the strength and/or offset of applied radio frequency (RF) fields.[6]

The time scale of the exchange process that can be studied using relaxation dispersion techniques is determined by the range of effective field strengths that can be applied.[3] For example, typically CPMG-type experiments use ν_{CPMG} fields ranging from 50 Hz to 1−2 kHz, where $\nu_{\mathrm{CPMG}} = 1/(2\tau)$ and τ is the delay between consecutive refocusing pulses. The methodology is thus well suited for the study of exchange processes on the millisecond time scale, with $k_{\mathrm{ex}} \approx 2\pi\nu_{\mathrm{CPMG}}$, where k_{ex} is the sum of forward and reverse rate constants for a two-site exchange process. In contrast, $R_{1\rho}$ measurements probe exchange events with $k_{\mathrm{ex}} \approx \omega_{\mathrm{e}}$ and most often employ relatively strong $\omega_1/(2\pi)$ fields of 1−2 kHz so that $\omega_{\mathrm{e}}/(2\pi)$ is in the range of ∼1−6 kHz ($\omega_{\mathrm{e}}^2 = \omega_1^2 + \delta^2$, with ω_1 the amplitude of the applied RF field and δ the offset of the resonance frequency Ω from the spin-lock carrier frequency Ω_{SL}). Because relatively large fields have been used in $R_{1\rho}$ experiments, it has generally been the case that $\omega_1^2 \gg \Delta\omega^2$, where $\Delta\omega$ is the frequency difference between the exchanging states. Moreover, most applications to date have focused on systems in the fast exchange limit, $k_{\mathrm{ex}}^2 \gg \Delta\omega^2$. In both limits, $\omega_1^2 \gg \Delta\omega^2$ or $k_{\mathrm{ex}}^2 \gg \Delta\omega^2$, it is not possible to extract all parameters describing a two-site conformational exchange from either $R_{1\rho}$[7] or CPMG data sets.[8]

In the past few years, there have been significant advances in the use of relaxation dispersion experiments for the study of protein dynamics. In the case of CPMG-based experiments,

[†] The University of Toronto.
[‡] Göteborg University.

(1) Fersht, A. *Structure and Mechanism in Protein Science*; W. H. Freeman and Company: New York, 1999.
(2) Alber, T.; Gilbert, W. A.; Ponzi, D. R.; Petsko, G. A. *Ciba Found. Symp.* **1983**, *93*, 4−24.
(3) Palmer, A. G.; Kroenke, C. D.; Loria, J. P. *Methods Enzymol.* **2001**, *339*, 204−238.
(4) Carr, H. Y.; Purcell, E. M. *Phys. Rev.* **1954**, *4*, 630−638.
(5) Meiboom, S.; Gill, D. *Rev. Sci. Instrum.* **1958**, *29*, 688−691.
(6) Deverell, C.; Morgan, R. E.; Strange, J. H. *Mol. Phys.* **1970**, *18*, 553−559.
(7) Korzhnev, D. M.; Orekhov, V. Y.; Dahlquist, F. W.; Kay, L. E. *J. Biomol. NMR* **2003**, *26*, 39−48.
(8) Ishima, R.; Torchia, D. A. *J. Biomol. NMR* **1999**, *14*, 369−372.

^{1}H,[9,10] ^{15}N,[11−13] and ^{13}C[14] single-quantum CPMG dispersion schemes that probe microsecond−millisecond dynamics at both backbone and side-chain positions in suitably labeled proteins have been supplemented by sequences in which decays of zero-,[10,15] double-,[10,15] and multiple-quantum[16] coherences are measured. It is thus possible to record a suite of six dispersion profiles for each backbone amide site, providing the opportunity to characterize exchange dynamics in some detail (in preparation). In the case of $R_{1\rho}$ measurements, a theoretical formalism has been developed that describes rotating frame relaxation outside the fast exchange limit,[17,18] and improved experimental schemes have been suggested that implement new methods for ^{1}H decoupling during the heteronuclear spin-lock period.[19,20] The basic features of the theory have been verified experimentally on a cavity mutant of T4 lyzosyme[21] that exchanges between two states with $k_{ex} \approx 1500\ s^{-1}$. Because spin-lock fields, $\omega_e/(2\pi)$, greater than 800 Hz were employed, $\omega_e^2 \gg k_{ex}^2$, it was not possible to independently separate k_{ex} from the populations of each of the exchanging states.[7] Separation of rates and populations in this case requires the use of significantly weaker ω_1 fields.

One of the main difficulties in using weak RF fields for $R_{1\rho}$ measurements is suppression of cross-correlation between dipole−dipole, chemical shift anisotropy interactions as well as elimination of evolution from *J*-coupling during the spin-lock. Very recently, new methodology for measurement of $R_{1\rho}$ relaxation with weak spin-lock fields has been proposed and demonstrated by Massi and co-workers,[20] with accurate values for ^{15}N $R_{1\rho}$ rates obtained using field strengths as low as 150 Hz. The ability to measure $R_{1\rho}$ rates with weak ω_1 fields is significant since it becomes possible, in principle, to extract all parameters of a two-state exchange process from a set of measurements at a single static magnetic field. That this is, in fact, the case is one of the central results of this article.

There are additional problems involving the application of low ω_1 fields, however. For nuclei with offsets $|\delta| \gg \omega_1$, measured $R_{1\rho}$ values have negligible contributions from transverse relaxation and, therefore, also from exchange, since in this limit $R_{1\rho} \approx R_1$. Moreover, it becomes increasingly difficult to align magnetization of different spins along their effective fields when spin-locking fields are weak.[20,22] It is therefore necessary to perform measurements on a limited set of nuclei, with similar heteronuclear resonance frequencies. In addition, because weak fields are employed, sampling of offsets must be fine, necessitating the measurement of a large number of 2D data sets. The extensive measurement of the spin-lock field and/or the offset dependence of $R_{1\rho}$ for multiple spins in a protein can be excessively time-consuming using conventional multidimensional techniques.

Here we describe a new experiment for measuring ^{15}N $R_{1\rho}$ values at weak spin-lock fields; fields as low as 25 Hertz have been employed. Rather than recording $R_{1\rho}$ rates using conventional 2D spectroscopy, we prefer to use a 1D scheme with selective Hartmann−Hahn polarization transfers[23,24] in which the relaxation properties of a single site are probed. Because only a single spin is queried, it is easy to completely suppress the effects of cross-correlation and *J*-coupling during the ^{15}N spin-lock using an *on-resonance* ^{1}H CW field, and magnetization alignment along the appropriate effective field is readily achieved by ^{15}N pulses with suitably tuned flip angles. The proposed methodology is applied to a G48M mutant of the Fyn SH3 domain, which exchanges between folded and unfolded states at 25 °C.[16,25] We show that off-resonance $R_{1\rho}$ rates measured at a single magnetic field strength allow independent extraction of all parameters of the exchange process. Advantages of the $R_{1\rho}$ technique over CPMG-type methods have also been noted for processes approaching the slow exchange limit.

Materials and Methods

Protein Sample. All $R_{1\rho}$ measurements were performed on an ^{15}N-labeled, perdeuterated, amide protonated (^{15}N/^{2}H) sample of the G48M mutant of the Fyn SH3 domain (0.8 mM in protein, 50 mM sodium phosphate, 0.2 mM EDTA, 0.05% NaN_3, 10% D_2O, pH 7), prepared as described previously.[16,26] It is noteworthy that the methodology can be equally well applied to protonated proteins.

NMR Spectroscopy. On- and off-resonance $R_{1\rho}$ experiments were carried out at 25 °C for selected ^{15}N nuclei of the ^{15}N/^{2}H G48M Fyn SH3 domain using Varian Inova spectrometers operating at field strengths of 14.1 and 18.8 T. The pulse sequence shown in Figure 1 and described below was employed. Selective Hartmann−Hahn polarization transfers from ^{1}H to ^{15}N and back[23,24] were performed with matched ^{1}H and ^{15}N CW fields $\omega_{1CP}/(2\pi) \approx 90$ Hz and with ^{1}H and ^{15}N carrier frequencies set to the resonance frequencies of the selected amide (measured with a high-resolution HSQC spectrum recorded prior to $R_{1\rho}$ measurements). ^{15}N RF field strengths were calibrated as described elsewhere.[27] The ^{1}H RF field strength used for cross polarization was adjusted to maximize the efficiency of magnetization transfer. On-resonance $R_{1\rho}$ experiments were performed at spin-lock field strengths $\omega_1/(2\pi)$ ranging from 25 Hz to 1 kHz in 25 Hz steps. Off-resonance experiments at each magnetic field were recorded with four to six spin-lock field strengths $\omega_1/(2\pi)$ ranging from 25 to 500 Hz and with 41−51 offsets selected individually for each spin. The minimal ω_1 value used in off-resonance experiments was chosen according to the chemical-shift difference between the exchanging states known from previous work[10,16,25] so that $R_{1\rho}$ rates recorded at the frequency of the minor state had measurable contributions from chemical exchange; offsets δ were selected so that the frequency range of the spin-lock carrier extends approximately from $\Omega_A + \omega_1$ to $\Omega_B - \omega_1$ ($\Omega_A > \Omega_B$) or $\Omega_B + \omega_1$ to $\Omega_A - \omega_1$ ($\Omega_B > \Omega_A$). All on- (off-)

(9) Ishima, R.; Torchia, D. *J. Biomol. NMR* **2003**, *25*, 243−248.
(10) Orekhov, V. Y.; Korzhnev, D. M.; Kay, L. E. *J. Am. Chem. Soc.* **2004**, *126*, 1886−1891.
(11) Loria, J. P.; Rance, M.; Palmer, A. G. *J. Biomol. NMR* **1999**, *15*, 151−155.
(12) Loria, J. P.; Rance, M.; Palmer, A. G. *J. Am. Chem. Soc.* **1999**, *121*, 2331−2332.
(13) Tollinger, M.; Skrynnikov, N. R.; Mulder, F. A. A.; Forman-Kay, J. D.; Kay, L. E. *J. Am. Chem. Soc.* **2001**, *123*, 11341−11352.
(14) Skrynnikov, N. R.; Mulder, F. A. A.; Hon, B.; Dahlquist, F. W.; Kay, L. E. *J. Am. Chem. Soc.* **2001**, *123*, 4556−4566.
(15) Dittmer, J.; Bodenhausen, G. *J. Am. Chem. Soc.* **2004**, *126*, 1314−1315.
(16) Korzhnev, D. M.; Kloiber, K.; Kay, L. E. *J. Am. Chem. Soc.* **2004**, *126*, 7320−7329.
(17) Trott, O.; Palmer, A. G. *J. Magn. Reson.* **2002**, *154*, 157−160.
(18) Abergel, D.; Palmer, A. G. *ChemPhysChem* **2004**, *5*, 787−793.
(19) Korzhnev, D. M.; Skrynnikov, N. R.; Millet, O.; Torchia, D. A.; Kay, L. E. *J. Am. Chem. Soc.* **2002**, *124*, 10743−10753.
(20) Massi, F.; Johnson, E.; Wang, C.; Rance, M.; Palmer, A. G., III. *J. Am. Chem. Soc.* **2004**, *126*, 2247−2256.
(21) Mulder, F. A. A.; Mittermaier, A.; Hon, B.; Dahlquist, F. W.; Kay, L. E. *Nat. Struct. Biol.* **2001**, *8*, 932−935.
(22) Mulder, F. A. A.; de Graaf, R. A.; Kaptein, R.; Boelens, R. *J. Magn. Reson.* **1998**, *131*, 351−357.
(23) Pelupessy, P.; Chiarparin, E.; Bodenhausen, G. *J. Magn. Reson.* **1999**, *138*, 178−181.
(24) Pelupessy, P.; Chiarparin, E. *Concepts Magn. Reson.* **2000**, *12*, 103−124.
(25) Korzhnev, D. M.; Salvatella, X.; Vendruscolo, M.; Di Nardo, A. A.; Davidson, A. R.; Dobson, C. M.; Kay, L. E. *Nature* **2004**, *430*, 586−590.
(26) Di Nardo, A. A.; Korzhnev, D. M.; Stogios, P. J.; Zarrine-Afsar, A.; Kay, L. E.; Davidson, A. R. *Proc. Natl. Acad. Sci. U.S.A.* **2004**, *101*, 7954−7959.
(27) Guenneugues, M.; Berthault, P.; Desvaux, H. *J. Magn. Reson.* **1999**, *136*, 118−126.

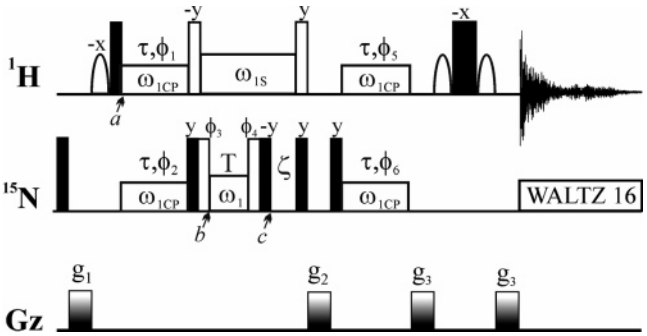

Figure 1. Selective 1D pulse scheme for recording on- and off-resonance $R_{1\rho}$ dispersions for backbone ^{15}N nuclei in proteins. Narrow (wide) filled rectangular pulses are applied with a tip angle of 90° (180°). Open ^{15}N (^{1}H) rectangular pulses are given with a tip angle of arccot($|\delta|/\omega_1$) (arccot($|\delta_W|/\omega_{1S}$)), where ω_1 is the ^{15}N spin-lock field strength, δ is the ^{15}N resonance offset from the spin-lock carrier, ω_{1S} is strength of the ^{1}H CW field applied during the ^{15}N spin-lock, and δ_W is the ^{1}H resonance offset from the frequency of water. The shaped proton pulses are selective for water (90°) and are typically implemented with "rectangular" shapes (~1.5 ms). The open rectangular boxes denote ^{15}N and ^{1}H spin-lock and CW irradiation periods. All high power pulses, water selective pulses, and spin-locks are given with phase *x* unless indicated otherwise. ^{15}N high power pulses are applied with a field of 5.8 kHz, with ^{15}N WALTZ16 decoupling[38] achieved using a 1 kHz field (at 14.1 T). ^{1}H high power pulses are applied with a 36 kHz field. Matched ^{1}H and ^{15}N CW fields, $\omega_{1CP}/(2\pi) \approx 90$ Hz, are applied during polarization transfer periods $\tau = 1/|J| \approx 10.8$ ms. A ^{1}H CW field, $\omega_{1S}/(2\pi) \approx 3900$ Hz, is used to suppress the effects of cross-correlation and *J*-coupling during the ^{15}N spin-lock period *T*. After the first water-selective pulse (phase $-x$), the ^{1}H carrier is moved to the amide resonance of interest and subsequently placed back on water prior to the water-gate element.[35] All ^{15}N rectangular pulses, along with the polarization transfer CW field (ω_{1CP}), are applied with the carrier set to the ^{15}N resonance frequency of the selected amide, whereas the ^{15}N spin-lock field (ω_1) is applied at an offset δ from the ^{15}N resonance. The optional delay ζ is discussed in the text. The phase cycle employed is as follows: ϕ_1 = {8(*y*),8(−*y*)}, ϕ_2 = {−*x*,*x*}; ϕ_5 = {4(*x*),4(−*x*)}; ϕ_6 = {2(*x*),2(−*x*)}; rec = {*x*,−*x*,−*x*,*x*, −*x*,*x*,*x*,−*x*, −*x*,*x*,*x*,−*x*, *x*,−*x*,−*x*,*x*}, for $\delta < 0$ (carrier downfield of resonance of interest) $\phi_3 = -y$ and $\phi_4 = y$; for $\delta > 0$ $\phi_3 = y$ and $\phi_4 = -y$. The durations and strengths of the gradients are as follows: g_1 (1ms,3G/cm), g_2 (50μs,15G/cm), g_3 (500μs,20G/cm).

resonance $R_{1\rho}$ experiments were performed in a constant-time manner, i.e., a series of 1D spectra were recorded at different ω_1 fields (offsets) with a constant relaxation period *T* of 30 (40) ms, along with a single reference spectrum with the spin-lock period *T* omitted. The 1D spectra were Fourier transformed, baseline corrected, and integrated using VNMR software. Peak integrals were converted into $R_{1\rho}$ rates according to $R_{1\rho} = -1/T \cdot \ln(I_1/I_0)$, where I_1 is the integral at $T = 30$ (40) ms, and I_0 the integral in the absence of the *T* period.[28] Errors in $R_{1\rho}$ rates were calculated from signal-to-noise ratios in 1D spectra. $R_{1\rho}$ measurements for different amides were performed using 96−256 transients and with a delay between scans of 1.1 s, ensuring signal-to-noise values of 50 to 150 in spectra obtained at $T = 0$. The resulting measuring times were 1.5 to 4.5 h per dispersion profile (40 to 50 points).

Theoretical Considerations. Consider an exchange process in which molecules interconvert between a ground state A and an excited conformation B with populations p_A and p_B, respectively, forward and reverse rate constants k_A and k_B ($k_A = k_{ex}p_B$, $k_B = k_{ex}p_A$, $k_{ex} = k_A + k_B$), and with a frequency separation between states of $\Delta\omega$. The evolution of magnetization in such a system due to chemical shift offset δ_i (i = A,B), the effects of an applied RF field of strength ω_1, as well as relaxation and chemical exchange, is given by the Bloch−McConnell equation[17,29] (see, for example, eq 4 of Trott and Palmer[17]). It can be shown for most cases of interest that the 6 × 6 matrix that describes the time evolution of the *X*, *Y*, and *Z* components of magnetization associated with states A and B has two real negative and four complex eigenvalues with large imaginary components. Thus, in principle, the evolution of magnetization during the spin-lock is given by the sum of six exponentials, $M(t) = M(0)\sum_i a_i \exp(\lambda_i t)$ ($\sum_i a_i = 1$). As described previously by Palmer and co-workers,[17] in many cases of experimental interest, all but one of the terms in the summation above are negligible. For example, the two real negative eigenvalues are often significantly different in magnitude,[17] with one very small (large in absolute value). In addition, for strong spin-lock fields the four terms that evolve with complex λ_i values deteriorate rapidly because of ω_1 field inhomogeneity. Thus, shortly after application of the spin-lock RF field five of the six components of $M(t)$ have decayed to zero so that the only remaining term relaxes monoexponentially with a rate given by the least negative real eigenvalue λ_1 of the matrix ($R_{1\rho} = -\lambda_1$). In the case of weak spin-lock fields ($\omega_1/(2\pi) \approx 100$ Hz, such as those applied in the present study), the ω_1 field inhomogeneity may not be sufficient to cause a rapid decay of the oscillatory terms (complex λ_i) that comprise $M(t)$. Simulations have established, however, that when magnetization from state A ($p_A \gg p_B$) is placed along the effective field given by the vector (ω_1,0,δ) at $t = 0$, the coefficients (a_i) of the complex terms are negligibly small. Thus, to excellent approximation the decay of magnetization is single exponential in the limit of weak applied spin-lock fields as well.

Although calculations of $R_{1\rho}$ are easily done numerically (see below), it is useful to consider the analytical expression for $R_{1\rho}$ so that the interplay between exchange parameters and ω_1, δ_i (i = A,B) can be better understood. An expression for $R_{1\rho}$ in the case of exchange occurring much faster than relaxation ($k_{ex} \gg R_1, R_2$) has been derived by Trott and Palmer:[17]

$$R_{1\rho} = R_1 \cos^2\theta + (R_2 + R_{ex}) \sin^2\theta \tag{1}$$

where

$$R_{ex} = \frac{p_A p_B \Delta\omega^2 k_{ex}}{\omega_{Ae}^2 \omega_{Be}^2/\omega_e^2 + k_{ex}^2} \tag{2}$$

$\theta = \text{arccot}(\delta_{av}/\omega_1)$, $\omega_{Ae}^2 = \omega_1^2 + \delta_A^2$, $\omega_{Be}^2 = \omega_1^2 + \delta_B^2$, $\omega_e^2 = \omega_1^2 + \delta_{av}^2$, $\delta_{av} = p_A\delta_A + p_B\delta_B$, and $\delta_A = \Omega_A - \Omega_{SL}$, $\delta_B = \Omega_B - \Omega_{SL}$ are resonance offsets from the spin-lock carrier for states A and B, respectively. In the asymmetric population limit, $p_A \gg p_B$, eq 2 can be written as:

$$R_{ex} = \frac{p_B \Delta\omega^2 k_{ex}}{\omega_{Be}^2 + k_{ex}^2} = \frac{p_B \Delta\omega^2 k_{ex}}{(\delta_A + \Delta\omega)^2 + \omega_1^2 + k_{ex}^2} \tag{3}$$

with $\Delta\omega = \Omega_B - \Omega_A$. In this limit $\delta_{av} \approx \delta_A$, so that the tilt angle θ in eq 1 is the angle between the direction of the effective field for state A and the *Z* axis. An important result from eq 3 is that for $p_A \gg p_B$ the maximum in R_{ex} occurs when the spin-lock field is resonant with the frequency of the minor state[17] (i.e., at an offset $\delta_A = \Omega_A - \Omega_{SL} = -\Delta\omega$ from the position of resonance of the major state).

Data Analysis. Measured ^{15}N $R_{1\rho}$ relaxation rates for selected residues of ^{15}N/^{2}H G48M Fyn SH3 were analyzed using a model in which exchange occurs between states A and B, as described above. Specifically, experimental $R_{1\rho}$ rates were fit to $R_{1\rho}$ values calculated from the Bloch−McConnell equation,[17,29]

$$d\mathbf{M}(t)/dt = \mathbf{R}\cdot\mathbf{M}(t) \tag{4}$$

where $\mathbf{R}$ is a 6 × 6 evolution matrix, $\mathbf{M} = (M_{AX}, M_{BX}, M_{AY}, M_{BY}, M_{AZ}, M_{BZ})^T$ is a vector consisting of the magnetization components for states A and B, and the superscript T denotes the transpose operation. $R_{1\rho}$ for magnetization in state A is calculated directly

(28) Mulder, F. A. A.; Skrynnikov, N. R.; Hon, B.; Dahlquist, F. W.; Kay, L. E. *J. Am. Chem. Soc.* **2000**, *123*, 967−975.
(29) McConnell, H. M. *J. Chem. Phys.* **1958**, *28*, 430−431.

from eq 4 according to

$$R_{1\rho} = -1/T\cdot\ln(\mathbf{u}\cdot\exp(\mathbf{R}T)\cdot\mathbf{v})$$

$$\mathbf{v}^{T} = \mathbf{u} = (\sin\theta, 0, 0, 0, \cos\theta, 0), \quad \theta = \operatorname{arccot}(\delta_{av}/\omega_1) \quad (5)$$

where **v** is a unit vector with elements proportional to the initial values of **M** (i.e., at the start of the spin-lock, **M**(0)), and **u** is a unit vector in the direction of the effective field of state A. Equation 5 holds for a spin-lock field applied along the *X* axis with the carrier at an offset of $\delta_{av}/(2\pi)$ Hz from the resonance position of spin A ($p_A \gg p_B$). In the derivation of eq 5, it is assumed that ^{15}N magnetization from state A only is present at the start of the spin-lock element since, as described below, a *selective* Hartmann−Hahn transfer of magnetization from ^{1}H to ^{15}N is employed. In principle, exchange during the magnetization transfer period can generate ^{15}N magnetization on state B as well. However, simulations have established that for the values of $\Delta\omega$ and k_{ex} in the present application this exchange transfer effect is small for the majority of the residues. In addition, we have assumed that the effective field for spin A is given by $(\omega_1,0,\delta_A)$. This assumption holds for spin-lock fields, ω_1, much greater than $R_2 - R_1$. A detailed analysis that includes the effects of relaxation (but neglects chemical exchange) shows that the direction of the effective field is given by $(\omega_1/(\omega_1^2 + \delta^2)^{1/2}, -(R_2 - R_1)\delta\omega_1/(\omega_1^2 + \delta^2)^{3/2}, \delta/(\omega_1^2 + \delta^2)^{1/2})$, for $(R_2 - R_1)/(\omega_1^2 + \delta^2)^{0.5} \ll 1$. For $(R_2 - R_1) = 10$ s^{-1}, $\omega_1/(2\pi) = 25$ Hz, the direction of the effective field is (0.82, −0.02, 0.58) (obtained with $\omega_1^2 = 2\delta^2$ for which the *Y* component is maximal); the assumption that the effective field is given by a vector along $(\omega_1,0,\delta_A)$ is thus quite reasonable, even for the low spin-lock fields used in this work.

Off-resonance $R_{1\rho}$ data measured at two magnetic fields and at 4−6 spin-lock fields were fit on a per residue basis with the following adjustable parameters: exchange rate constant k_{ex}, population of the minor state p_B, (signed) chemical shift difference, in parts per million, between the exchanging states $\Delta\varpi$ ($\Delta\omega = 10^{-6}\gamma_N B_0 \Delta\varpi$, where $\Delta\omega$ is the frequency difference between the exchanging states, γ_N is the ^{15}N gyromagnetic ratio, and B_0 is the static magnetic field strength) and intrinsic transverse (R_2) and longitudinal (R_1) relaxation rates at 14.1 and 18.8 T. We have assumed that the intrinsic relaxation properties are the same for spins in each of the two states. It can be shown[30] that in the limit that $p_A \gg p_B$ the position of the major conformer is at $\Omega_A' = \Omega_A + p_B k_{ex}^2 \Delta\omega/(k_{ex}^2 + \Delta\omega^2)$; in the case of the ^{15}N/^{2}H G48M Fyn SH3 domain, however, the differences between Ω_A' and Ω_A are reasonably small (<7.6 Hz for $\Delta\varpi > 2$ ppm, $p_B = 0.05$, $k_{ex} = 400$ s^{-1}, 18.8 T field) and in what follows we have assumed that $\Omega_A' = \Omega_A$ and therefore that $\delta_A = \Omega_A' - \Omega_{SL}$. Different combinations of off-resonance $R_{1\rho}$ data measured at different magnetic fields and spin-lock values were fit together to establish what the minimum experimental data set is (in the present case) for which accurate exchange parameters can be extracted. On-resonance $R_{1\rho}$ data for each residue measured at two magnetic fields were fit together with five adjustable parameters: k_{ex}, p_B, $\Delta\varpi$ along with R_2 at 14.1 and 18.8 T. Correlation coefficients between the extracted exchange parameters and uncertainties of the parameters were calculated using the covariance matrix method.[31] Parameters from $R_{1\rho}$ data analyses were compared to those obtained from fits of single-quantum ^{15}N CPMG data measured using the same sample and analyzed as described previously.[16]

Constant-Time vs Non-Constant-Time Experiments. As described above, $R_{1\rho}$ values have been obtained by measuring peak integrals (state A) with and without a constant time period of duration *T* and $R_{1\rho}$ calculated as $-1/T\cdot\ln(I_1/I_0)$. Obtaining $R_{1\rho}$ values from a single *T* period has the advantage that a large number of offsets (ω_1 fields) can be explored. A disadvantage, however, is that while the decay of the spin-locked magnetization becomes effectively single-exponential shortly after application of the spin-lock, $M(T) = a_1 M(0)\exp(\lambda_1 T)$, (see discussion above), the coefficient, a_1, varies with the offset of the ^{15}N spin-lock carrier from the resonance positions of spins in states A and B. *The offset dependence of the prefactor a_1 is a function of the initial state of magnetization at $T = 0$.* In the experiments performed here, to good assumption, only magnetization associated with state A is present at the start of the spin-lock period, because of the selective nature of the Hartmann−Hahn transfer that precedes it (see discussion below). During the spin-lock period, a rapid equilibration of magnetization can ensue (with a time constant on the order of $1/k_{ex}$), with the ratio of magnetization of states A and B approaching p_A/p_B, so long as the magnetization vectors for the two states are (near) collinear. Consider, for example, the case of an $R_{1\rho}$ experiment where the ^{15}N carrier is far off-resonance so that magnetization from states A and B have large components along the *Z* axis (and hence magnetization vectors are collinear). Exchange leads to a rapid equilibration of magnetization so that the magnetization associated with state A approaches $p_A M(0)$, where $M(0)$ is the initial magnetization in state A. Subsequent evolution of magnetization in state A is well described by $M(T) = p_A M(0)\exp(\lambda_1 T)$ (i.e., $a_1 = p_A$). A similar situation occurs in the case of transverse magnetization associated with state A so long as the chemical shift difference between sites A and B is small. In contrast, if the carrier is on-resonance for state A, and $\Delta\omega$ is large, magnetization is transferred from A to B because of exchange (i.e., lost from state A), but there is little *net* magnetization returned (since the phase relation between magnetization in states A and B varies rapidly in time). In this case, the magnetization of state A does not rapidly proceed to $p_A M(0)$, and simulations show that $M(T) = M(0)\exp(\lambda_1 T)$ (i.e., $a_1 = 1$). The offset dependence in *a* is fully taken into account in eq 5, using the appropriate initial conditions for **M**(0). Notably, values of $R_{1\rho}$ estimated on the basis of a single *T* value according to $-1/T\cdot\ln(I_1/I_0)$, differ from $-\lambda_1$ (the least negative eigenvalue of the Bloch−McConnell exchange matrix), with the differences increasing for large values of offsets from the spin-lock carrier. The value of $R_{1\rho}$ can be related to $-\lambda_1$ via the empirical relation $-1/T\cdot\ln(I_1/I_0) = -\lambda_1 - 1/T\cdot\ln(a_1)$, where $a_1 = 1 - p_B\cos^2(\theta_A - \theta_B)$, $\theta_A = \operatorname{arccot}(\delta_A/\omega_1)$, $\theta_B = \operatorname{arccot}(\delta_B/\omega_1)$, with approximate expressions for $-\lambda_1$ derived by Trott and Palmer,[17] as discussed above. The offset dependence of $R_{1\rho}$ estimated from this empirical formula reproduces almost exactly the dependence obtained from eq 5. Of interest, we have found that in the case of CPMG experiments the pre-exponent describing the decay of magnetization varies with CPMG frequency, ν_{CPMG}, so that $R_{2,eff}$ (CPMG) values generated from a single constant-time experiment are related to R_2 rates calculated from the Carver and Richards equation[32] through a correction term as well.[16]

As described above, the correction that must be applied to $R_{1\rho}$ values obtained from data sets recorded with a single constant-time spin-lock period depends on the initial conditions at the start of the spin-lock. With a slight modification of the sequence of Figure 1, it is possible to change the initial conditions so that the magnetization associated with states A and B reflects the equilibrium distribution (i.e., p_A, p_B). This can be achieved by insertion of a delay (on the order of $1/k_{ex}$) after the first 90_y ^{15}N pulse (when magnetization is along the *Z* axis) that allows equilibration to occur. Simulations have established that in this case correction of $R_{1\rho}$ values is not necessary (i.e., to good approximation $R_{1\rho}$ is given by $-\lambda_1$), and although this approach was not used in the present study, it has been verified experimentally. Finally, in the case of experiments where $R_{1\rho}$ values are estimated on the basis of several *T* points (non-constant-time experiments), the decay rate, $-\lambda_1$, is extracted directly from the *T* dependence of magnetization intensity. Thus, initial conditions of magnetization are not required for the analysis, and a correction factor is unnecessary (i.e., $R_{1\rho}$ value measured directly from the decay of magnetization is $-\lambda_1$).

(30) Skrynnikov, N. R.; Dahlquist, F. W.; Kay, L. E. *J. Am. Chem. Soc.* **2002**, *124*, 12352−12360.
(31) Press, W. H.; Flannery, B. P.; Teukolsky, S. A.; Vetterling, W. T. *Numerical Recipes in C*; Cambridge University Press: Cambridge, 1988.
(32) Carver, J. P.; Richards, R. E. *J. Magn. Reson.* **1972**, *6*, 89−105.

Results and Discussion

NMR Experiment for Measurement of $R_{1\rho}$. Figure 1 illustrates the 1D NMR pulse scheme that has been developed for recording on- and off-resonance $R_{1\rho}$ dispersions of backbone ^{15}N nuclei in proteins with low spin-lock fields. The experiment is based on selective excitation of amide resonances using Hartmann−Hahn polarization transfers with weak CW fields and is designed to measure ^{15}N $R_{1\rho}$ rates for one NH group at a time. The excitation scheme used in the experiment is similar to that described by Bodenhausen and co-workers.[23] At the beginning of the pulse sequence equilibrium, ^{15}N magnetization is destroyed by the first ^{15}N 90° pulse and the gradient g1. Subsequently, transverse ^{1}H magnetization, $-H_Y$, is created (point *a*) and transferred to $\pm N_X$ using matched ^{1}H and ^{15}N on-resonance CW fields, ω_{1CP}, by adjusting the phases ϕ_1 and ϕ_2, respectively. The CW fields are applied for a duration of $\tau = 1/|J|$ (where $J \approx -93$ Hz is the HN scalar coupling constant; here we use $\omega_{1CP}/(2\pi) \approx 90$ Hz; see below). Prior to the application of the ^{15}N spin-lock of length *T* (point *b*), nitrogen magnetization is aligned along the direction of the effective field in the rotating frame given by the vector $(\omega_1,0,\delta_A)$ using a pair of ^{15}N pulses, $90°_y\theta°_{\phi 3}$, $\theta = \text{arccot}(|\delta_A|/\omega_1)$, with ω_1 the spin-lock field strength and δ_A the resonance offset of the major state from the spin-lock carrier. The effects of *J*-coupling and cross-correlation between dipole−dipole and CSA relaxation mechanisms are suppressed during the ^{15}N spin-lock by a strong ^{1}H CW field $\omega_{1S} > \omega_1$ ($\omega_{1S}/(2\pi) \approx 4$ kHz) applied on-resonance for the spin of interest. After the spin-lock period *T*, ^{15}N magnetization is returned to the *X* axis by a $\theta°_{\phi 4}$ $90°_{-y}$ pulse pair ($\phi 3 = -\phi 4$, point *c*) and transferred back to protons for observation. (The optional delay ζ will be described below.)

It is well-known that presaturation or dephasing of the water resonance can cause significant sensitivity losses in NMR experiments,[33] and we have measured intensity decreases on the order of 30−40% for the G48M Fyn SH3 domain. The pulse sequence of Figure 1 is designed to minimally perturb the solvent magnetization. Thus, a water-selective pulse is applied before the first ^{1}H nonselective pulse so that at point *a* the water magnetization is aligned along the $+Z$ axis. Application of a weak ^{1}H CW field, ω_{1CP}, used to transfer polarization from ^{1}H to ^{15}N (and back) has a minimal effect on water magnetization provided that $\omega_{1CP} \ll |\delta_W|$, where δ_W is the amide ^{1}H resonance offset from the frequency of water (i.e., carrier offset from water). This condition is not maintained for the ^{1}H CW field, ω_{1S}, used to suppress the effects of *J*-coupling and cross-correlation during the ^{15}N spin-lock period *T*, since ω_{1S} is chosen to be larger than ω_e, $\omega_e^2 = \omega_1^2 + \delta_A^2$, to avoid the Hartmann−Hahn matching condition.[34] Therefore, water magnetization during this period is preserved by locking it along the direction of the ^{1}H effective field in the rotating frame given by $(\omega_{1S},0,\delta_W)$ using a ^{1}H pulse of phase $-y$ and flip angle of $\text{arccot}(|\delta_W|/\omega_{1S})$. After ^{1}H CW irradiation, the water magnetization is returned to the $+Z$ axis in a similar manner. Any remaining water magnetization in the transverse plane is destroyed by gradient g_2 and the water-gate block[35] so that flat baselines and hence accurate peak integrals can be obtained.

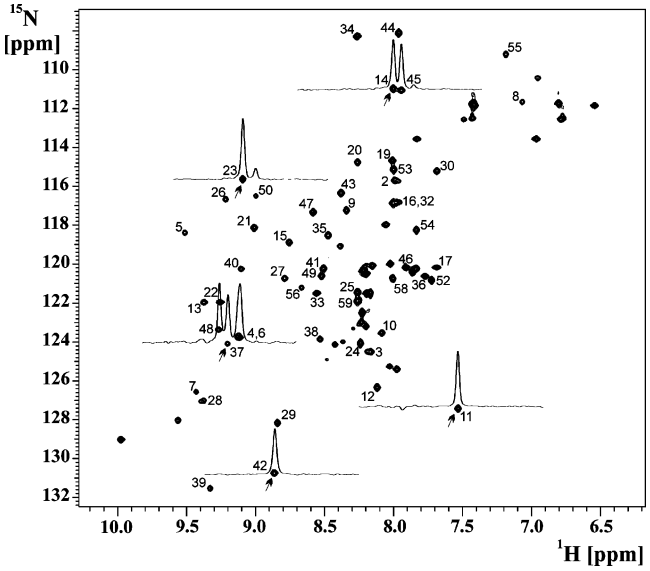

Figure 2. ^{1}H−^{15}N correlation spectrum of the ^{15}N/^{2}H G48M mutant of the Fyn SH3 domain, 18.8 T, 25 °C, with cross-peaks labeled by residue number. 1D spectra for the amide groups of Glu 11, Thr 14, Gly 23, Trp 37, and Leu 42 obtained using the pulse sequence of Figure 1 are shown, with the positions of the ^{1}H,^{15}N carriers for the selective Hartmann−Hahn transfers indicated by arrows (on-resonance for a given residue).

To obtain accurate $R_{1\rho}$ rates using the scheme of Figure 1, very selective Hartmann−Hahn transfers are required since only 1D amide proton spectra are recorded. Pelupessy and co-workers have shown that polarization can be *completely* transferred between ^{1}H and ^{15}N spins in $\tau = 1/|J|$ using weak fields, $\omega_{1CP} = \pi J\sqrt{4n^2-1}/2$, where *n* is a positive integer.[23,24] However, so long as there is very little mismatch between ^{1}H and ^{15}N fields, the transfer efficiency is high for any value of $\omega_{1CP}/(2\pi)$ larger than $|J|\sqrt{3}/4$.[24] To minimize losses due to conformational exchange during transfer periods, we suggest using the highest ω_{1CP} field that ensures good selectivity with little dephasing of water magnetization (here we have used $\omega_{1CP}/(2\pi) \approx 90$ Hz). It is worth noting that for ^{15}N and ^{1}H RF fields on the order of 90 Hz the transfer efficiency is not very sensitive to mismatch in fields so long as the mismatch does not exceed 5%.

Figure 2 shows a 2D ^{1}H−^{15}N correlation plot of the G48M Fyn SH3 domain recorded at a field strength of 18.8 T, along with 1D spectra obtained using the scheme of Figure 1. The selectivity of each 1D spectrum depends on the strength of the Hartman−Hahn field (ω_{1CP}) used in polarization transfers. Offset profiles for the efficiency of cross-polarization are given by Pelupessy and Chiarparin;[24] for $\omega_{1CP}/(2\pi) \approx 90$ Hz, correlations outside approximately $\pm 1.5|J|$ Hz from the ^{1}H/^{15}N carriers are completely suppressed. In general, one can *selectively* excite the resonance of interest if its separation from neighboring peaks along either the ^{15}N or ^{1}H dimension exceeds $\sim 1.5\omega_{1CP}/(2\pi)$ (for example, Leu 42, Glu 11, and Gly 23 in Figure 2). Of course, for the experiments proposed here, where ^{1}H chemical shifts are recorded, separation of correlations in the ^{1}H dimension is sufficient, irrespective of the degree of overlap in ^{15}N (see, for example, Trp 37 or Thr 14 in Figure 2). In cases where correlations have the same ^{1}H, but different ^{15}N frequencies, residuals from unwanted signals (in the 1D ^{1}H spectrum) may affect the measured $R_{1\rho}$ rates (unless the separation in the ^{15}N dimension is larger than $\sim 1.5\omega_{1CP}/(2\pi)$ Hz). If the selectivity

(33) Grzesiek, S.; Bax, A. *J. Am. Chem. Soc.* **1993**, *115*, 12593−12594.
(34) Ernst, R. R.; Bodenhausen, G.; Wokaun, A. *Principles of Nuclear Magnetic Resonance in One and Two Dimensions*; Oxford University Press: Oxford, 1987.
(35) Piotto, M.; Saudek, V.; Sklenar, V. *J. Biomol. NMR* **1992**, *2*, 661−665.

of the Hartmann−Hahn polarization transfers is not sufficient, a purge element can be included in the scheme of Figure 1 to eliminate the unwanted signal. This is achieved through the addition of a delay $\zeta = \pi/(2\delta)$, where $\delta/(2\pi)$ is the offset (Hz) of the unwanted peak from the resonance of interest. During the period ζ, the magnetization of interest remains along X, while the magnetization that is to be eliminated rotates by 90° (to the Y axis) and is subsequently dephased by gradient g_2.

At first glance, it might seem that measuring relaxation rates one residue at a time is inefficient relative to a 2D approach, and indeed for many applications (^{15}N R_1, R_2, and ^{1}H−^{15}N steady state NOE, for example) this is, of course, true. However, in studies of chemical exchange outside the fast regime, it is often necessary to use weak spin-lock fields to extract the full complement of parameters describing the exchange process (see below), and many of the advantages normally associated with 2D measurements (i.e., specifically that all residues can be studied at once) are lost. For example, measurement of $R_{1\rho}$ relaxation rates requires that magnetization be spin-locked along the appropriate effective field (which varies as a function of ^{15}N chemical shift). This is often done using adiabatic pulses,[22] but such pulses become prohibitively long, and concomitant relaxation losses significant, in cases where the spin-lock field is weak. An alternative approach makes use of a pulse/free precession element.[36,37] However, alignment errors become significant for $|\delta|/\omega_1 > 0.4$.[20] Thus, even if a series of 2D spectra were recorded, only magnetization associated with correlations confined to relatively small regions of chemical shift would be effectively locked, necessitating acquisition of a large number of data sets to obtain a complete set of relaxation rates. Further, a complete sampling of the offset-dependence of $R_{1\rho}$ is predicated on offset increments significantly less than the strength of the spin-lock field, again requiring that a large number of data sets be acquired. In some cases, this could be prohibitive. The advantages of the proposed 1D scheme are several-fold. First, in many applications only a select number of residues report on the exchange event, and these residues can be studied far more effectively by 1D NMR. In many cases, these residues may be identified readily by recording CPMG dispersion experiments with a small number of ν_{CPMG} values. Once the resonances are identified, a series of 1D $R_{1\rho}$ measurements can be performed at a number of B_1 fields using a relatively small number of offsets to estimate exchange parameters prior to a more careful analysis for which the approximate exchange values are useful. Second, the experiment time can be adjusted appropriately for each amide, along with the optimal selection of spin-lock fields and/or offsets. Third, it is straightforward to spin-lock magnetization using pulses with appropriately adjusted flip angles, and unlike the approach that makes use of adiabatic pulses, the procedure is effectively instantaneous. Fourth, because residues are queried one at a time, cross-correlation and scalar coupling effects can be suppressed simply by on-resonance ^{1}H CW decoupling. In the case of 2D applications, more complex schemes are required.[19,20] Finally, as described above, dephasing of water can be minimized very effectively in the present scheme; this is more difficult to accomplish efficiently in the case of 2D approaches, and notably, methods in the literature at the present time dephase water completely.[19,20]

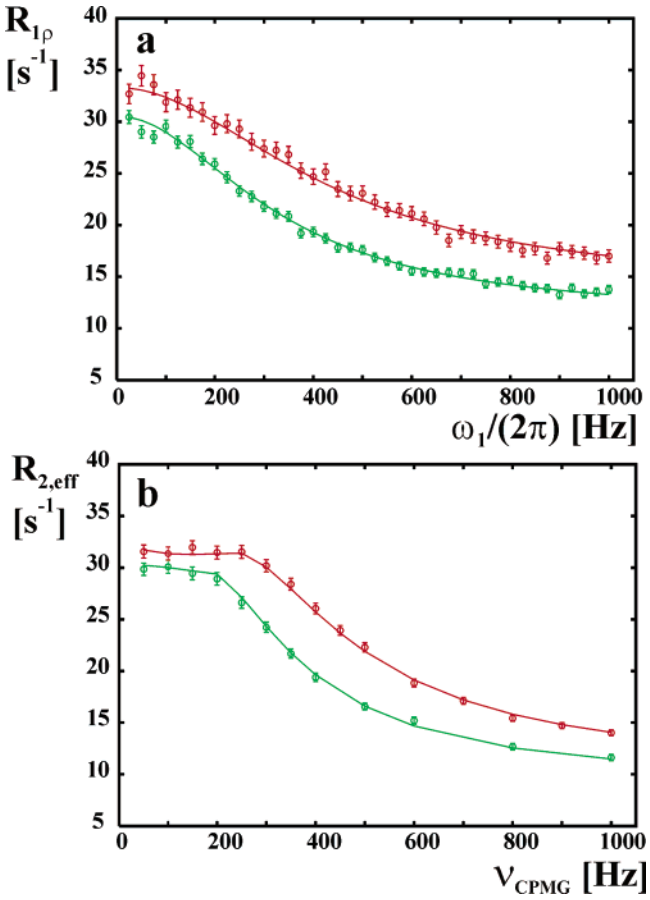

Figure 3. Experimental on-resonance ^{15}N $R_{1\rho}$ (a) and $R_{2,\text{eff}}$ CPMG (b) dispersion profiles (○) and best fits (solid curves) for Glu 11 of G48M Fyn SH3, as a function of the applied spin-lock field $\omega_1/(2\pi)$ ($R_{1\rho}$ data) or pulse repetition frequency ν_{CPMG} ($R_{2,\text{eff}}$ CPMG data). Profiles measured at magnetic fields of 14.1 and 18.8 T are shown in green and red, respectively.

Application to the G48M Fyn SH3 Domain. The pulse sequence described above (Figure 1) has been applied to measure the exchange dynamics of a G48M mutant of the SH3 domain from the Fyn tyrosine kinase. This domain has been shown by a variety techniques, including fluorescence spectroscopy[26] and CPMG-based NMR relaxation dispersion methods,[10,16,25,26] to exchange between folded and unfolded states. Very recently, we have shown that the exchange process involves an intermediate state,[25] but in what follows here a two-state model of folding will be used to analyze the data. Our previous work made use of ^{15}N/^{1}H samples of G48M and G48V mutants of the Fyn SH3 domain, and at 25 °C the populations of the intermediate (I) and unfolded (U) states were determined to be 1.2, 2% and 1.8, 5% for the G48M and G48V mutants, respectively.[25] In contrast, at 25 °C a similar three-site exchange analysis for the deuterated G48M sample considered here shows that the I and U states are at populations of 0.7 and 5%, respectively (in preparation). Thus, the level of the I state is significantly reduced with respect to the U state in the deuterated sample, and a two-state analysis is adequate for what we wish to discuss here. A more detailed analysis will follow. ^{15}N, ^{1}H single-quantum, zero- and double-quantum, and multiple-quantum CPMG dispersion experiments (six types of dispersion

(36) Griesinger, C.; Ernst, R. R. *J. Magn. Reson.* **1987**, *75*, 261−271.
(37) Yamazaki, T.; Muhandiram, R.; Kay, L. E. *J. Am. Chem. Soc.* **1994**, *116*, 8266−8278.
(38) Shaka, A. J.; Keeler, J.; Frenkiel, T.; Freeman, R. *J. Magn. Reson.* **1983**, *52*, 335−338.

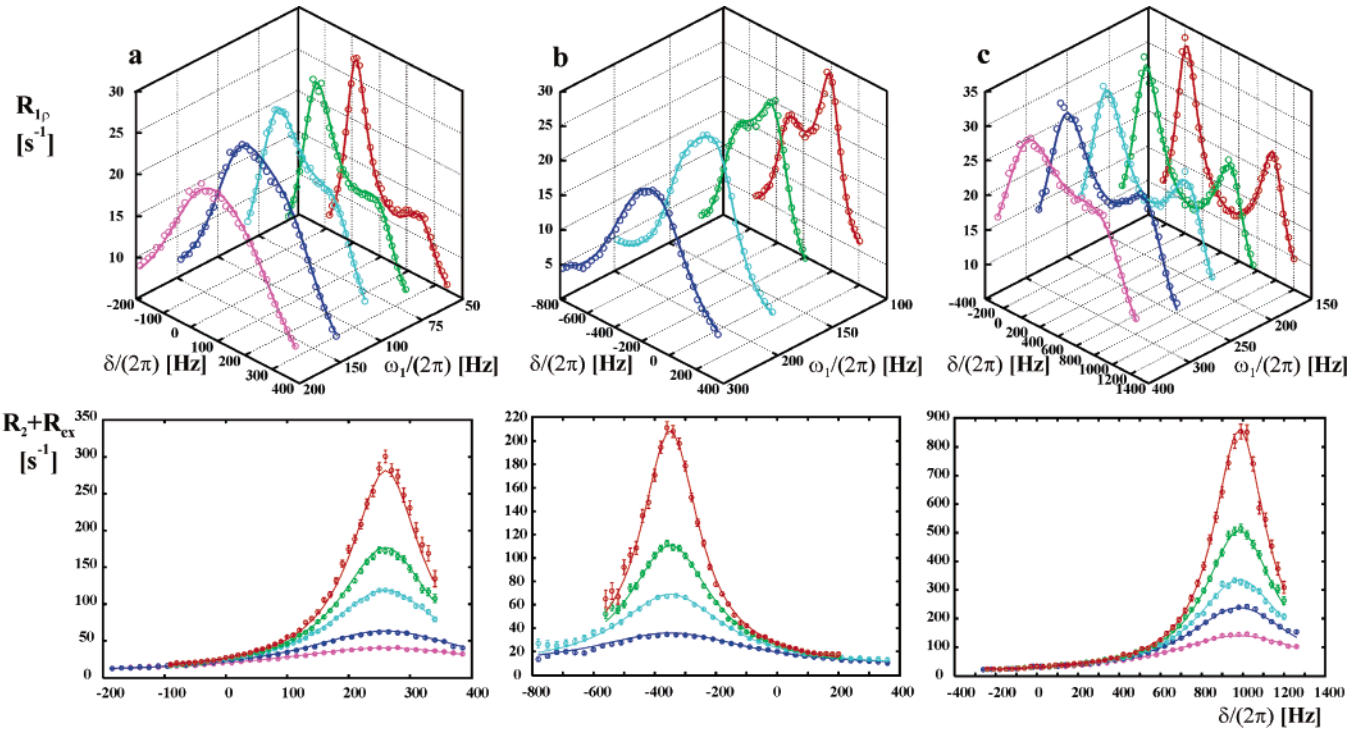

Figure 4. Experimental off-resonance ^{15}N $R_{1\rho}$ profiles (○) and best fits (solid lines) for Thr 14 (a), Glu 11 (b), and Val 55 (c) measured at a magnetic field of 14.1 T (top plots), and the corresponding $R_{ex} + R_2$ contributions to $R_{1\rho}$, bottom plots, $(R_{1\rho} + 1/T\cdot\ln(a_1) - R_1 \cos^2\theta)/\sin^2\theta$, where $a_1 = 1 - p_B \cos^2(\theta_A - \theta_B)$, $\theta_A = \text{arccot}(\delta_A/\omega_1)$, $\theta_B = \text{arccot}(\delta_B/\omega_1)$ as a function of resonance offset from the spin-lock carrier $\delta/(2\pi) \approx \delta_A/(2\pi)$. The best fit parameters were obtained from fits of the $R_{1\rho}$ offset profiles to eq 5. The color coding for the different spin-lock fields $\omega_1/(2\pi)$ (indicated in the top plots) is used in the bottom plots as well. All data for a given residue, four or five spin-lock fields at each of two static magnetic fields (14.1 and 18.8 T) are fit simultaneously (data recorded at 18.8 T not shown).

profiles have been measured for 47 residues, each at three magnetic fields) have been recorded on the ^{15}N/^{2}H sample used in the present study, 25 °C. A fit of this extensive data set to a two-site exchange model gives $k_{ex} = 377\ s^{-1}$, $p_B = 5.2\%$, and these parameters are used as a reference to evaluate the accuracy of values extracted from the $R_{1\rho}$ data sets.

Figure 3a shows experimental on-resonance ^{15}N $R_{1\rho}$ dispersion profiles (open circles) for Glu 11 of G48M Fyn SH3 ($|\Delta\varpi| \approx 5.8$ ppm) recorded at magnetic fields of 14.1 and 18.8 T, along with best fits of the data (solid curves). By means of comparison, ^{15}N single-quantum CPMG dispersion profiles for the same residue are shown in Figure 3b. On-resonance ^{15}N $R_{1\rho}$ profiles have been measured at spin-lock field strengths, $\omega_1/(2\pi)$, ranging from 25 Hz to 1 kHz in steps of 25 Hz, corresponding approximately to the range of ν_{CPMG} frequencies that have been used in the ^{15}N CPMG experiment. Similar on-resonance $R_{1\rho}$ and $R_{2,eff}$ CPMG dispersion profiles for Glu 11 are obtained, with a difference of approximately 15 s^{-1} between $R_{1\rho}$ ($R_{2,eff}$) values at the lowest and highest $\omega_1/(2\pi)$ (ν_{CPMG}) fields. As predicted by eqs 1−3, the on-resonance $R_{1\rho}$ vs $\omega_1/(2\pi)$ profile is Lorentzian. Note that the maximum spin-lock field strength that can be applied in ^{15}N $R_{1\rho}$ experiments depends on the length, T, of the spin-lock period. At $T = 30-40$ ms, $\omega_1/(2\pi)$ fields up to 2−2.5 kHz can be safely employed (although we did not use spin-lock fields higher than 1 kHz in this work). Thus, the range of $\omega_1/(2\pi)$ fields accessible to on-resonance ^{15}N $R_{1\rho}$ measurements (from ∼10−20 Hz to 2−2.5 kHz) is approximately a factor of 2 larger than the range of ν_{CPMG} frequencies normally used in ^{15}N single-quantum CPMG experiments (50 Hz−1 kHz). It is noteworthy that any value of spin-lock field $\omega_1/(2\pi)$ from the range indicated above can be used in the $R_{1\rho}$ experiment. In contrast, in constant relaxation time CPMG experiments ν_{CPMG} frequencies can only be sampled at certain values. For example, in a typical ^{15}N single-quantum CPMG experiment with two constant time periods, each of duration 20 ms[28] and separated by an element that interconverts inphase and antiphase ^{15}N magnetization,[12] the smallest multiple of ν_{CPMG} that can be employed is 50 Hz.

Figure 4a−c shows experimental off-resonance ^{15}N $R_{1\rho}$ profiles (open circles) and best fits (solid lines) as a function of offset from the spin-lock carrier $\delta \approx \delta_A$ for Thr 14 ($\Delta\varpi \approx 4.3$ ppm), Glu 11 ($\Delta\varpi \approx -5.8$ ppm), and Val 55 ($\Delta\varpi \approx 16.2$ ppm) measured at 14.1 T (top plots), and the corresponding $R_{ex} + R_2$ contributions to $R_{1\rho}$ calculated as $(R_{1\rho} + 1/T\cdot\ln(a_1) - R_1 \cos^2\theta)/\sin^2\theta$, where $a_1 = 1 - p_B \cos^2(\theta_A - \theta_B)$, $\theta_A = \text{arccot}(\delta_A/\omega_1)$, and $\theta_B = \text{arccot}(\delta_B/\omega_1)$ (bottom plots). As described above, each value of $R_{1\rho}$ is calculated using only one value of T. We have verified, however, that the decay of ^{15}N magnetization as a function of T is exponential (starting from T values of a few milliseconds), with the profile of the intensity of Thr 14 vs time shown in Figure 5 obtained using a spin-lock field of 100 Hz (on-resonance and at ±100 Hz off-resonance). Note that the decay profiles are very different for the two offsets (±100 Hz). In the absence of exchange or if the time scale of the exchange process was very fast, identical decays would be expected.

In the absence of exchange, the offset profile of $R_{1\rho}$ has a maximum at and is symmetric about $\delta_A = 0$, with a characteristic width on the order of ω_1 (eq 1). In the case of exchange between a populated state A and a minor conformation B, $R_{1\rho}$ profiles are modified by the exchange contribution R_{ex} to R_2 that exhibits a maximum at the position of state B (eqs 2 and

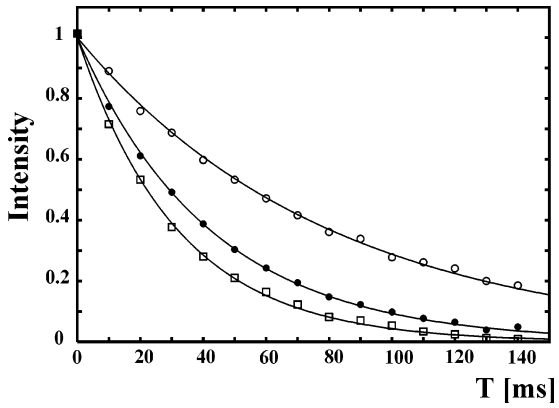

Figure 5. Decay of spin-locked magnetization for Thr14 of the G48M Fyn SH3 domain, 18.8 T, 25 °C as a function of T (in intervals of 10 ms) using 100 Hz spin-locking fields with offsets of 0 (□), +100 (●), and −100 (○) Hz.

3), resulting in an asymmetric offset dependence of $R_{1\rho}$ (Figure 4). Thus, off-resonance $R_{1\rho}$ profiles for Thr 14 (Figure 4a) have a single maximum shifted toward the position of the minor state ($\delta/(2\pi) \approx 260$ Hz) at $\omega_1/(2\pi)$ of 150 and 200 Hz, and they develop a flat shoulder extending from $\delta/(2\pi) \approx 100$ to 300 Hz for $\omega_1/(2\pi)$ values of 50, 75, and 100 Hz. Similar profiles are observed for Glu 11 (Figure 4b), but at the lowest $\omega_1/(2\pi)$ of 100 Hz used for this residue the second $R_{1\rho}$ maximum becomes clearly visible at the position of the minor state ($\delta/(2\pi) \approx -350$ Hz). Most striking are the $R_{1\rho}$ profiles for Val 55, for which an unusually large $\Delta\varpi$ is observed: 16.2 ppm (Figure 4c). For $\omega_1/(2\pi)$ fields ranging from 150 to 300 Hz, the $R_{1\rho}$ profiles show two distinct maxima of comparable amplitude, one at the position of state A ($\delta/(2\pi) \approx 0$ Hz) and the other near the frequency of the minor state B ($\delta/(2\pi) \approx 980$ Hz), where the contribution of $R_{ex} + R_2$ to $R_{1\rho}$ is scaled by the factor $\sin^2\theta \approx (\omega_1/\delta)^2$ (equal to 0.023 at $\omega_1/(2\pi)$ of 150 Hz). As expected from eqs 2 and 3, profiles for R_{ex}, extracted from $R_{1\rho}$ data (bottom plots in Figure 4), have Lorentzian shapes, centered at the positions of the minor state B, and for low values of $\omega_1/(2\pi)$ the line widths of the profiles are determined by the exchange rate constant k_{ex}.

A potential point of confusion in any comparison of R_{ex} values measured from CPMG and $R_{1\rho}$ data sets relates to the definition of R_{ex} in both cases. In the case of CPMG measurements, one can define $R_{ex}(\nu_{CPMG})$ as $R_{2,eff}(\nu_{CPMG}) - R_{2,eff}(\infty)$.[8] That is, $R_{ex}(\nu_{CPMG})$ is the contribution to R_2 from the exchange process at a given ν_{CPMG} value. In contrast, the contribution to $R_{1\rho}$ from exchange is given by $R_{ex}\sin^2\theta$. Thus, in the case of the G48M Fyn SH3 domain, values of R_{ex} at the frequency of state B ($\Omega_{SL} = \Omega_B$, $\delta_A = -\Delta\omega$) typically exceed $R_{ex}(0)$ values measured in either on-resonance $R_{1\rho}$ ($\Omega_{SL} = \Omega_A$, $\delta_A = 0$) or CPMG experiments by 1−2 orders of magnitude. For example, the value of $R_{ex} + R_2$ at $\Omega_{SL} = \Omega_B$ is approximately 300 s^{-1} for Thr 14 at $\omega_1/(2\pi) = 50$ Hz, 210 s^{-1} for Glu 11 at $\omega_1/(2\pi) = 100$ Hz and 850 s^{-1} for Val 55 at $\omega_1/(2\pi) = 150$ Hz (14.1 T magnetic field). Clearly the only reason that one can observe such fast rates is that R_{ex} is scaled by $\sin^2\theta$, a value that is small for large offsets from the resonance of the major state, $\delta_A \gg \omega_1$.

Table 1 presents the extracted exchange parameters from on- and off-resonance $R_{1\rho}$ data for Thr 14, Glu 11, and Val 55 of $^{15}N/^2H$ G48M Fyn SH3, 25 °C, along with a comparison of parameters extracted from ^{15}N single-quantum CPMG dispersion data. For these three residues, $k_{ex}^2 \ll \Delta\omega^2$ (slow exchange), and in this limit the off-resonance experiments are particularly powerful in relation to their on-resonance and CPMG counterparts. For example, when on-resonance $R_{1\rho}$ and CPMG data sets are fit, values of $k_{ex}(p_B)$ for these residues are in error by several hundred s^{-1} (several percent), with a correlation coefficient between k_{ex} and p_B always less than −0.99 (greater than 0.99 in absolute value, data not shown). Only if p_B is fixed to a value of 5% (obtained from fits of CPMG dispersion profiles from 47 residues, see above) are reasonable values of k_{ex} obtained, without any loss in the quality of fits (see Table 1; note that on-resonance $R_{1\rho}$ and $R_{2,eff}$ CPMG data do not provide the sign of $\Delta\varpi$). In addition, parameters extracted from off-resonance $R_{1\rho}$ data sets for a number of additional residues are also presented in the table. For all the residues, exchange parameters have been obtained from fits using eq 5 (see Materials and Methods section). It is worth mentioning that if the offset dependence of $R_{1\rho}$ (measured from single constant time experiments) is fit to the empirical relation $-\lambda_1 - 1/T\cdot\ln(a_1)$, where $a_1 = 1 - p_B\cos^2(\theta_A - \theta_B)$, $\theta_A = \text{arccot}(\delta_A/\omega_1)$, $\theta_B = \text{arccot}(\delta_B/\omega_1)$, parameters very close to those obtained using eq 5 are obtained. Finally, if the offset dependence of $R_{1\rho}$ is fit to $-\lambda_1$ similar parameters are obtained, with slight differences in p_B and k_{ex} noted (but with overestimation of R_1 values extracted from the fits).

In contrast to fits of on-resonance $R_{1\rho}$ and $R_{2,eff}$ CPMG profiles where only a limited set of exchange parameters are available in the slow exchange limit, extraction of all parameters can be obtained from fits of off-resonance $R_{1\rho}$ data, even for residues with extremely large $\Delta\omega$ values (i.e., for Val 55 with $\Delta\varpi = 16.2$ ppm; see Table 1). This is possible by recording $R_{1\rho}$ rates using a spin-lock field on the order of k_{ex} placed near the frequency of the minor state B so that $\delta_A + \Delta\omega \approx 0$ (see eq 3). It is worth mentioning in this context that the offset dependence of R_{ex} (eqs 2 and 3; Figure 4, bottom plots) can be related in a simple way to the parameters of a two-site conformational exchange process. The position of the R_{ex} maximum with respect to the frequency of the major state A defines the value of $\Delta\omega$ (and its sign), with the width and amplitude of the R_{ex} profile related to k_{ex} and p_B, respectively.

More insight into the sensitivity of CPMG-based dispersion profiles and off-resonance $R_{1\rho}$ curves to exchange parameters can be obtained by comparing eq 3 with a simple approximate expression[8] that has been proposed for the exchange contribution R_{ex} to $R_{2,eff}$ in CPMG experiments that reproduces the exact rates within 15% for all exchange regimes if $p_B/p_A < 0.15$:

$$R_{ex} = \frac{p_A p_B \Delta\omega^2 k_{ex}}{\sqrt{\omega_{1,eff}^4 + p_A^2\Delta\omega^4} + k_{ex}^2}. \qquad (6)$$

In eq 6 $\omega_{1,eff} = 12^{1/2}\nu_{CPMG} \approx 3.46\nu_{CPMG}$, $\nu_{CPMG} = 1/(2\tau)$, with τ the delay between successive refocusing pulses. Equations 3 and 6 share many common features. For example, in the fast exchange limit, $k_{ex} \gg |\Delta\omega|$, and/or in the limit of large spin-lock (CPMG) fields ω_1 ($\omega_{1,eff}$) $\gg |\Delta\omega|$, the $\Delta\omega$ terms in the denominators of eqs 2, 3, and 6 are negligible. Thus, the only parameters that can be extracted from fits of the ω_e dependence of $R_{1\rho}$ or the $\omega_{1,eff}$ dependence of $R_{2,eff}$ in the case of CPMG data are k_{ex} and the product $p_A p_B \Delta\omega^2$ (which is the only combination of p_A, p_B, and $\Delta\omega$ in eqs 2, 3, and 6 in this case).

Table 1. Conformational Exchange Parameters Obtained from Least-Square Fits of Different Sets of On-Resonance ($R_{1\rho}$ On) and Off-Resonance ($R_{1\rho}$ off) Rotating Frame Relaxation Data for Thr 14, Glu 11, and Val 55 of the $^{15}N/^{2}H$ Labeled G48M Fyn SH3 Domain (25 °C), along with Exchange Parameters Obtained from Fits of ^{15}N Single-Quantum CPMG Dispersion Data Recorded at 14.1 and 18.8 T[a]

	data set	k_{ex} (s^{-1})	p_B (%)	$\Delta\varpi$ (ppm)
T14	$R_{1\rho}$ off: 14.1 T (50, 75, 100, 150, 200 Hz) 18.8 T (100, 200, 400 Hz)	345 ± 6	6.05 ± 0.09	4.30 ± 0.01
	$R_{1\rho}$ off: 14.1 T (50, 75, 100, 150, 200 Hz)	331 ± 5	6.02 ± 0.08	4.28 ± 0.01
	$R_{1\rho}$ off: 14.1 T (50, 75 Hz)	346 ± 8	5.82 ± 0.09	4.28 ± 0.01
	$R_{1\rho}$ off: 14.1 T (50 Hz)	365 ± 8	5.94 ± 0.09	4.32 ± 0.02
	$R_{1\rho}$ on: 14.1, 18.8 T	395 ± 5	5.00 (f)	4.19 ± 0.10*
	$R_{2,eff}$ CPMG: 14.1,18.8 T	396 ± 5	5.00 (f)	4.41 ± 0.06*
E11	$R_{1\rho}$ off: 14.1 T (100, 150, 200, 300 Hz) 18.8 T (100, 150, 200, 400 Hz)	379 ± 12	5.78 ± 0.16	−5.78 ± 0.01
	$R_{1\rho}$ off: 14.1 T (100, 150, 200, 300 Hz)	356 ± 17	5.97 ± 0.25	−5.78 ± 0.02
	$R_{1\rho}$ off: 14.1 T (100, 150 Hz)	326 ± 18	6.26 ± 0.30	−5.79 ± 0.02
	$R_{1\rho}$ off: 14.1 T (100 Hz)	279 ± 23	7.01 ± 0.51	−5.74 ± 0.02
	$R_{1\rho}$ on: 14.1, 18.8 T	426 ± 4	5.00 (f)	5.60 ± 0.11*
	$R_{2,eff}$ CPMG: 14.1, 18.8 T	437 ± 4	5.00 (f)	5.86 ± 0.07*
V55	$R_{1\rho}$ off: 14.1 T (150, 200, 250, 300, 400 Hz) 18.8 T (200, 250, 300, 400, 500 Hz)	316 ± 20	6.88 ± 0.44	16.21 ± 0.02
	$R_{1\rho}$ off: 14.1 T (150, 200, 250, 300, 400 Hz)	308 ± 24	7.00 ± 0.56	16.22 ± 0.02
	$R_{1\rho}$ off: 14.1 T (150, 200 Hz)	373 ± 31	5.93 ± 0.44	16.24 ± 0.03
	$R_{1\rho}$ off: 14.1 T (150 Hz)	323 ± 53	6.66 ± 0.96	16.24 ± 0.04
	$R_{1\rho}$ on: 14.1, 18.8 T	398 ± 54	5.00 (f)	18.34 ± 2.22*
	$R_{2,eff}$ CPMG: 14.1, 18.8 T	374 ± 23	5.00 (f)	15.49 ± 0.35*
G23	$R_{1\rho}$ off: 14.1 T (100, 150, 200, 300 Hz) 18.8 T (100, 150, 200, 400 Hz)	355 ± 12	5.77 ± 0.17	−6.14 ± 0.01
L29	$R_{1\rho}$ off: 14.1 T (25, 50, 75, 100, 150, 200 Hz) 18.8 T (75, 100, 200 Hz)	437 ± 12	5.17 ± 0.07	−1.93 ± 0.02
W37	$R_{1\rho}$ off: 14.1 T (75, 100, 150, 200 Hz) 18.8 T (75, 100, 200 Hz)	423 ± 17	5.37 ± 0.13	−2.79 ± 0.02
A39	$R_{1\rho}$ off: 14.1 T (100, 150, 200, 300 Hz)	428 ± 16	4.92 ± 0.15	−7.30 ± 0.02
L42	$R_{1\rho}$ off: 14.1 T (100, 150, 200, 300 Hz) 18.8 T (100, 150, 200, 400 Hz)	449 ± 12	4.65 ± 0.10	−6.22 ± 0.01
T44	$R_{1\rho}$ off: 14.1 T (100, 150, 200, 300 Hz) 18.8 T (100, 150, 200, 400 Hz)	444 ± 12	4.75 ± 0.10	6.03 ± 0.01

[a] Additionally, exchange parameters are shown extracted from off-resonance $R_{1\rho}$ data for Gly 23, Leu 29, Trp 37, Ala 39, Leu 42, and Thr 44. Static magnetic fields and spin-lock fields $\omega_1/(2\pi)$ (for off-resonance $R_{1\rho}$ data only) at which the data have been collected are listed under "data set". On-resonance $R_{1\rho}$ data and CPMG data were fit with the population of the minor state, p_B, fixed to 5.0%, marked by the letter f (see text for discussion). Values of $\Delta\varpi$ from fits of on-resonance $R_{1\rho}$ or CPMG data (marked by *) are unsigned. Uncertainties in the exchange parameters were calculated from the covariance matrix of the optimized model.[31]

In contrast, in the limit where $k_{ex}^2 \ll \omega_1^2 + \Delta\omega^2$, only $\Delta\omega$ and $k_A = k_{ex}p_B$ can be obtained from on-resonance $R_{1\rho}$ (eq 3, $\Omega_{SL} = \Omega_A$, $\delta_A = 0$, at $p_A \gg p_B$) or from CPMG data, eq 6 ($k_{ex}^2 \ll \sqrt{\omega_{1,eff}^4 + p_A^2\Delta\omega^4}$), even for small values of ω_1. However, it is still possible to extract all exchange parameters in this case from *off-resonance* $R_{1\rho}$ measurements so long as $\omega_1 \approx k_{ex}$ and provided that $R_{1\rho}$ values are well sampled near the frequency of the minor state B ($\Omega_{SL} = \Omega_B$, $\delta_A = -\Delta\omega$) and that the contribution of $(R_2 + R_{ex})\sin^2\theta$ to $R_{1\rho}$ is still measurable at this frequency (see eq 1). In this regard, the present experiment is complementary to CPMG approaches. A protocol in which dispersion profiles are first generated using CPMG-based experiments, followed by selective off-resonance $R_{1\rho}$ measurements for residues whose exchange parameters cannot be fully obtained in this manner, is likely to be appropriate in many applications.

Finally, to establish what the minimal $R_{1\rho}$ data set might be for the extraction of accurate exchange parameters, several different combinations of off-resonance $R_{1\rho}$ data collected at different magnetic field and spin-lock field strengths were fit for a number of the residues in Table 1. It appears that there is no need to record an extensive off-resonance $R_{1\rho}$ data set at multiple static magnetic field strengths. In fact, values of k_{ex} and p_B, deviating by no more than 35% from reference values obtained from fits involving extensive CPMG data sets, were obtained from data measured at a single spin-lock field strength $\omega_1 \approx k_{ex}$ and at a single magnetic field.

In summary, we have presented a new selective 1D ^{15}N $R_{1\rho}$ experiment for the measurement of rotating frame relaxation rates in proteins at low spin-lock fields $\omega_1/(2\pi)$, with values as low as 25 Hz tested. The experiment is designed to study one resonance at a time using selective excitation with Hartmann−Hahn polarization transfers at low matched ^{1}H and ^{15}N CW fields. The methodology has been applied to an $^{15}N/^{2}H$ labeled sample of the G48M mutant of the Fyn SH3 domain which exchanges between folded and unfolded states. A number of advantages of this experiment relative to on-resonance $R_{1\rho}$ and CPMG measurements have emerged. Specifically, it is shown that even in the limit where $\Delta\omega \gg k_{ex}$ it is possible to extract accurate parameters characterizing the exchange process in a two-site exchanging system from off-resonance dispersion profiles recorded at spin-lock fields $\omega_1 \approx k_{ex}$. The ideas described in this article may be applied to the design of other selective 1D relaxation dispersion experiments, and work along these lines is currently in progress.

Acknowledgment. This research was supported by a grant from the Canadian Institutes of Health Research (C.I.H.R.) to L.E.K. D.K. acknowledges the C.I.H.R. for a postdoctoral fellowship. We are grateful to members of the laboratory of Professor Alan Davidson (University of Toronto) for preparation of the sample used in this work. L.E.K. holds a Canada Research Chair in Biochemistry.

JA0446855